SPE 613

Water Coning Control in Oil Wells by Fluid Injection

CHARLES R. SMITH
JUNIOR MEMBER AIME
SYLVAIN J. PIRSON
MEMBER AIME

THE U. OF TEXAS
AUSTIN, TEX.

ABSTRACT

The effect of fluid injection to control water coning in oil and gas wells was investigated. Analytical and model techniques were employed. The factors investigated were the position and length of the completion interval, the point of fluid injection, the viscosity of the injected fluid and the relative thickness of the oil and water sections. The resulting influence of these factors on the net producing water-oil ratio was determined.

Several important conclusions can be drawn from the study. In general, it was found that the net producing water-oil ratio can be reduced by fluid injection. The magnitude of this reduction depended on the factors listed above. An important practical consideration is that the injection fluid may be either oil or water. If the injected fluid is less dense than the connate water of the reservoir, the fluid will not be lost. This fact is reassuring when valuable oil is being injected. Efforts to suppress water production were more successful when the injection fluid was more viscous than the reservoir oil, or when a zone of reduced permeability existed in the vicinity of the point of fluid injection. Under test conditions, little benefit was derived through the use of impermeable barriers or cement "pancakes".

INTRODUCTION

The occurrence of water coning has been known for at least 60 years. In thin oil or gas pay sections, the presence of an oil-water or gas-water contact hinders production and often causes early abandonment of the afflicted well if a completion is even attempted. Even when relatively thick pay sections are found, the encroachment of water when a water drive is present will eventually pose serious water coning problems. This water is often corrosive, expensive to separate from the oil or gas and is costly to dispose of.

The theory of water coning has been discussed by a number of authors.[1,2,3,4] Briefly, water coning to the producing interval in a well is due to pressure gradients resulting from the production of fluid from the reservoir. These pressure gradients will cause a water cone to rise toward the bottom of the producing interval if a water-oil or water-gas contact exists. The tendency of the water to cone is offset or partially offset by gravity forces since the water has a higher specific gravity than the oil. A balance then exists between two forces, gravitational forces arising from the difference in specific gravities of the oil and water, and the pressure gradients causing the flow of fluids to the wellbore. If the pressure gradient exceeds the gravitational force, water coning to the wellbore occurs and water production results.

Through the years considerable thought has been given to the water coning problem. More than 50 U. S. Patents have been granted to inventors on the subject. A relatively complete literature review of the water coning problem has been made.[5] A number of these patents hold considerable promise for the solution or the partial solution of the water and/or the coning problem. Very little has been written describing field tests of techniques for the suppression of water coning. A notable exception is the paper by West.[6] He reports success in reducing gas coning by a combination of gravel packing and oil injection above the oil-producing interval. He also describes a comparable method to prevent water coning, but provides no field examples.

This study experimentally and analytically verifies the benefits of oil injection as a means of partially or completely suppressing the water cone. While the gas coning problem was not treated, it is anticipated that results comparable to those obtained in water suppression could be obtained with reduced oil injection since the viscosity contrast between oil and gas exceeds that between oil and water. For the purpose of this study, the conventional potential flow theory was applied to the water-coning problem. The experimental verification centered on both a radial and a linear model. The model study permitted the investigation of complex flow configurations and the use of fluids of differing densities and viscosities. No analytic expressions are available to permit a solution of the problem as stated (see Fig. 1).

Original manuscript received in Society of Petroleum Engineers office April 1, 1963. Revised manuscript received Oct. 1, 1963.

[1]References given at end of paper.

POTENTIAL FLOW THEORY AND APPLICATION TO THE WATER-CONING PROBLEM

Most analytical approaches to the fluid-flow problem have been based upon the methods of classical hydrodynamics, a branch of applied mathematics which deals with the perfect or ideal fluid. This hypothetical fluid is incompressible and non-viscous by definition. In addition, the fluid can slip along its boundaries without resistance. Despite these very limiting assumptions, the potential flow theory of classical hydrodynamics permits the solution of many practical problems in fluid dynamics. It is possible to develop expressions for the streamlines and isopotential lines for a number of cases of two-dimensional fluid flow of interest in the water-coning problem. It is also possible to add two or more flow coning patterns to obtain solutions of more complex systems. This procedure has been followed to develop analytical expressions applicable to water coning and to the injection of fluid to reduce water producing rates.

Fig. 2 is a plot of the flow streamlines from a uniform source to a point sink in a two-dimensional system. The analytical expression for the stream function is:[7]

$$\psi = \frac{-2Q}{\pi} \arctan \left[\tanh \frac{\pi x}{2L} \tan \frac{\pi y}{2L} \right] \quad \ldots\ldots\ldots\ldots (1)$$

Appendix contains the derivation for flow from the mid point to upper side of a two-dimensional system. Fig. 3 shows the configuration of the necessary source and sink and the resulting streamlines. Eq. 18 describes the analytical expression. In plotting the figures, a multiplying factor of 1,000 has been used to avoid fractional values. The height L of the system was taken as being one. The assigned value of Q was π.

The above-mentioned analytical equation can be added in any proportion and still satisfy the Laplace equation, i. e., is analytic and is a harmonic function. In order to compare the results of the analytical development with an experimental oil and water system,[5] the strength of the source of Fig. 3 was reduced from unity to 0.396, and added to the value of the stream function plotted in Fig. 2. The resulting flow configuration is shown in Fig. 4. The injection-point source strength was calculated by noting that in the experimental system (Table 3 of Ref. 5), the uniform source flow rate of reservoir oil and water totalled 0.929 cc/sec. The injection-oil point source strength was 0.368 cc/sec. The $\psi = 0$ line represents the boundary between the flow from the uniform source to the right of the figure and the flow from the source at the mid point of the left side of the system. If, for the purpose of visualization, the $\psi = 1{,}000$ line were considered to be the water-oil contact, then the resulting flow configuration would represent the injection of fluid slightly above the original oil-water contact for the case where there is zero density difference between the oil and water.

Fig. 5 was plotted to provide a comparison of the experimentally and analytically derived cone shapes and the corresponding injection fluid profiles. The analytical cone shape for the zero fluid density difference was traced by using the same inlet cone height as in the experimental case. Since the oil-water contact is a streamline, the shape of the cone could be traced in by paralleling

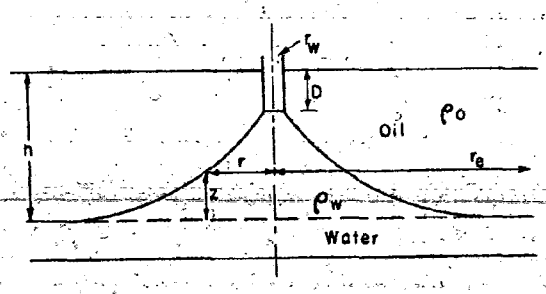

FIG. 1 — SKETCH OF WATER CONE.

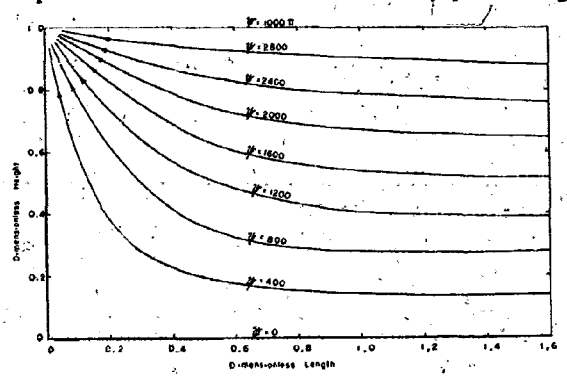

FIG. 2 — FLOW STREAMLINES FROM UNIFORM SOURCE TO POINT SINK — TWO-DIMENSIONAL SYSTEM.

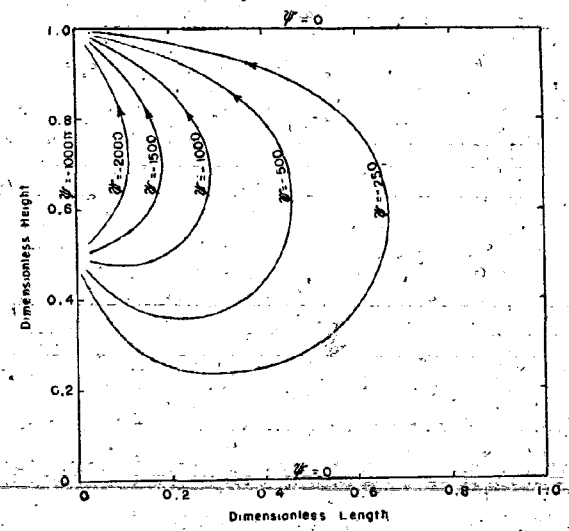

FIG. 3 — FLOW STREAMLINES FROM POINT SOURCE AT MID POINT TO POINT SINK — TWO-DIMENSIONAL SYSTEM.

the streamlines plotted in Fig. 4.

Fig. 5 demonstrates the gravitational forces which act when fluids of different densities are used. When no density difference between the fluids exists, the cusp of water to the producing interval is of considerable width. This creates a large cross-sectional area through which water may flow. When the lower fluid (water) is more dense than the upper fluid (oil), the injection of a fluid (oil) at the same rate as in the zero density difference case results in a smaller cross sectional area for the flow of water to the producing interval. In the experimental system the injection and reservoir oils had viscosities and densities of 2.18 cp and 0.826 (39.8°API), respectively. The water had a viscosity of 0.905 cp and a density of 1.0078. As might be expected, the greater the density difference between the oil and water of the practical case, the smaller will be the water producing rate for a given oil producing rate.

An interesting feature of Fig. 5 is the position of the lower boundary of the injection fluid for the zero and the finite-density difference cases. Where gravity is effective, the injection oil is buoyed up (the dashed curve). From this, one would expect that the injection of oil of the same specific gravity as the reservoir water should result in the position of the lower part of the boundary approximately coinciding with the curve shown for the zero-density difference case (the solid line).

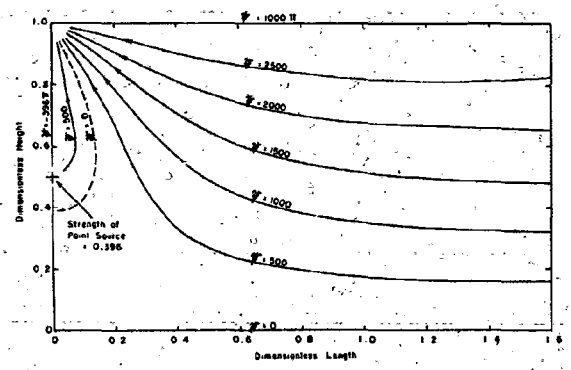

FIG. 4 — FLOW STREAMLINES FROM UNIFORM SOURCE AND POINT SOURCE OF REDUCED STRENGTH AT MID POINT TO POINT SINK — TWO-DIMENSIONAL SYSTEM.

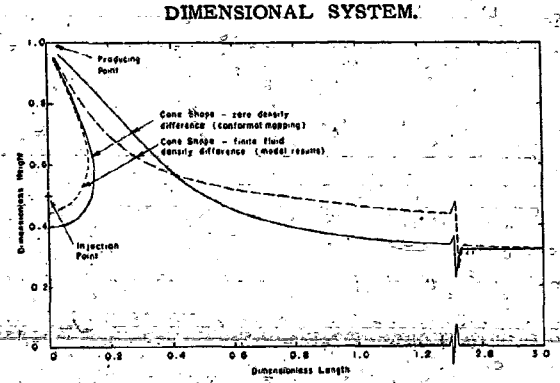

FIG. 5 — WATER CONE SHAPES IN A TWO-DIMENSIONAL SYSTEM—COMPARISON OF MODEL AND ANALYTICAL RESULTS.

It may also be observed from Fig. 5 that the negative slope of the oil-water contact to the right of the diagram is larger when there is a difference in the densities of the two fluids. This interface shape is necessary for dynamic equilibrium of the oil and water sections when the flow of the water has been reduced by gravitational forces and/or by fluid injection. This is evident from consideration of the situation existing when the water cone is at the maximum possible height for water-free oil production. If the water is at rest with oil flowing above toward the producing interval, then a finite slope of the oil-water contact must exist. A pressure differential is present both in the oil layer and in the water layer when the oil is flowing. If the water is at rest, then the pressure differential must be reflected as the slope of the oil-water contact.

In the cases where there is no density contrast between the fluids, flow will occur at every point in the system except at the stagnation points. In this case, a horizontal interface can exist at a distance from the producing interval.

The preceding observations can be concisely stated as follows: If water is a rest at infinity, then a horizontal interface and a horizontal, irrotational (non-zero) oil flow cannot both exist.

The preceding discussion for flow in the two-dimensional system, leads to several pertinent comments that could be made regarding flow in a radial system. The change of pressure with respect to radius dp/dr in the radial system is inversely proportional to the radius $1/r$. This means that at a large distance from the wellbore, the pressure gradient would be extremely small. This pressure gradient is even smaller for the case where the well has only partial penetration into the fluid-producing section of the reservoir. This indicates that while it is impossible to avoid the existence of a finite slope of the oil-water contact, superimposing a flow system by fluid injection at the wellbore can be effective as a means for water-cone suppression. The slope would be slightly increased at a distance from the wellbore due to this increased flow, but it would be of negligible magnitude. This increase of slope would satisfy the requirement that, if the oil is flowing, then either a slope of the water-oil interface must exist or the water must flow to the producing interval.

SHAPE OF THE WATER CONE

Analytic solutions for the shape of the water cone where no water is flowing have appeared recently in the literature. Karp, Lowe and Marusov[8] have developed an expression for water-cone shape in a radial system with partial penetration of the oil zone. The authors had also derived the equation independently in slightly different form:

$$Z = h - \sqrt{h^2 + \frac{(h^2 - D^2)\ \ln r/r_e}{\ln r_e/r_w}} \qquad (2)$$

Interestingly, the predicted cone shape does not give an exact representation of the cone shape observed in the radial model water-coning experiments of this study. The lack of agreement between the observed and calculated cone shapes may be traced to a very limiting assumption made in the development of the cone shape equation, Eq. 2. It was assumed that the production of oil was due to the pressure gradient in the radial direction r. In the vicinity of the well, where the producing interval only partially penetrates the oil-bearing section, the actual flow has an important vertical component. The exact solution would, then, of course, consider the vertical pressure gradient also. A direct analytical solution may not be possible where the vertical pressure gradient is also considered.

Karp, *et al*, have also developed an expression for the water cone shape in a two-dimensional system:

$$Z = h - \sqrt{h^2 - \frac{(h^2 - D^2)\ (r_e - r)}{r_e - r_w}} \quad \ldots\ldots\ldots\ldots (3)$$

Comparison of the shape of the cone to that obtained in the two-dimensional coning studies by models shows reasonably good agreement of the general shapes.

The authors think that a more nearly correct shape of the water cone for the radial and two-dimensional cases could be obtained by a trial-and-error technique. The case where a producing water-oil ratio is present could also be treated. The procedure would be to assume a cone shape by using the cone shape equation of Karp, *et al*, as a first approximation. Since the pressure must be zero on the oil-water contact and along the entire cone shape, the use of Bernouilli's equation would permit the calculation of the actual pressure in both the oil and water sections at the oil-water interface. If the calculated values in the oil and water sections do not agree at the contact, then the interface would be adjusted by trial-and-error until the solution for the cone shape resulted. When the position of the cone had been established, then relaxation techniques could be applied to determine the potential and streamlines of the flow in both the water and oil sections, if required. It should be possible to treat the case where oil or water is injected in the same wellbore to suppress water coning. The above suggested trial-and-error technique has not been used in this study.

It should also be possible to extend the above trial-and-error technique to the case where the ratio of the horizontal to the vertical permeability is not unity. This directional property may be taken into account by graphing with the horizontal dimensions reduced by the factor $\sqrt{k_v / k_h}$. k_v and k_h are the vertical and horizontal permeabilities, respectively. In sand reservoirs, the horizontal permeability may be from 2 to 100 times the permeability in the vertical direction.

In this study, the shape of the water cone, with and without fluid injection, has been treated by using a two-dimensional model and a radial model. The primary advantage of a model study is that complex flow configurations may be investigated and fluids of differing densities and viscosities may be used. No analytic expressions which permit a solution of the formulated problem are available at the present time.

WATER CONING STUDY WITH THE HELE-SHAW MODEL

THEORETICAL BASIS AND SCALING FACTORS

Basically, the Hele-Shaw[9,10] model consists of two closely-spaced parallel plates. The analogy is based on the correspondence between the flow of fluid through a porous media and the laminar flow of a viscous fluid between the two closely-spaced plates. The principles of viscous flow analogy are well known. For very low fluid velocities between parallel plates, the velocity distribution is parabolic. The mean velocity across the interspace is proportional to the pressure gradient so that

$$v_x = -k \frac{\partial P}{\partial x} \qquad v_y = -k \frac{\partial P}{\partial y}$$

The continuity equation in the xz plane is

$$\frac{\partial v_x}{\partial x} + \frac{\partial v_y}{\partial y} = 0$$

Therefore:

$$\frac{\partial^2 p}{\partial x^2} + \frac{\partial^2 p}{\partial y^2} = 0 \quad \ldots\ldots\ldots (4)$$

where x and y refer to the rectangular coordinate system. The pressure is then analogous to the velocity potential of an irrotational flow system.

The problem treated in this study involves the simultaneous flow of two liquids segregated by gravity forces. The permeability (expressed in darcies) is the same in either of the fluids, $w^2/12$, where w is the plate spacing in centimeters. The equation for flow between two closely-spaced parallel plates may then be written four times:

$$q_{om} = \frac{w^3{}_m}{12} \quad \frac{\gamma_m \quad \rho_{om}}{\nu_{om}} \quad \frac{dp}{dr_m} \ ,$$

$$q_{op} = \frac{w^3{}_p}{12} \quad \frac{\gamma_p \quad \rho_{op}}{\nu_{op}} \quad \frac{dp}{dr_p} \quad \ldots\ldots\ldots\ldots (5)$$

$$q_{wm} = \frac{w^3_m}{12} \frac{y_m \quad \rho_{wm}}{\nu_{wm}} \frac{dp}{dr_m}$$

$$q_{wp} = \frac{w^3_p}{12} \frac{y_p \quad \rho_{wp}}{\nu_{wp}} \frac{dp}{dr_p}$$

Imposing the condition that the water-oil ratio with the corresponding producing rates be equal in the model and the prototype, it follows directly that:[11]

$$\frac{\nu_{wm}}{\nu_{om}} = \frac{\nu_{wp}}{\nu_{op}} \quad \ldots\ldots\ldots (6)$$

In addition, the pressure along the interface must be the same in either fluid, therefore:

$$p_{wm}\ (r_m, z) + \rho_{wm}\, g z_m = p_m\ (r_m, z_m = 0) \quad \ldots\ldots\ldots (7)$$

$$p_{om}\ (r_m, z) + \rho_{om}\, g(z_m - Z_m) + \rho_{wm}\ g z_m = p_m(r_m, z_m = 0) \quad \ldots\ldots\ldots (7a)$$

Combining and rearranging Eqs. 7 and 7a (noting that $p_o = p_w$ if capillary pressure is neglected) results in:

$$\frac{\rho_{wm}}{\rho_{om}} z_m = z_m - Z_m \left[\frac{\rho_{om} - \rho_{wm}}{\rho_{om}}\right] \quad \ldots\ldots (8)$$

Similarly, the corresponding equation for the prototype is:

$$\frac{\rho_{wp}}{\rho_{op}} z_p = z_p - Z_p \left[\frac{\rho_{op} - \rho_{wp}}{\rho_{op}}\right] \quad \ldots\ldots (9)$$

It follows directly that the choice of the liquids will be controlled by the relation:

$$\left[\frac{\rho_o - \rho_w}{\rho_o}\right]_m = \left[\frac{\rho_o - \rho_w}{\rho_o}\right]_p \quad \ldots\ldots\ldots (10)$$

Since a capillary interspace between the two plates is involved, the capillary rise must be considered.[11] However, because the thickness of the oil and water sections were much larger than the capillary rise, the capillary effect proved to be negligible in the experiments conducted. No attempts were made to scale the length and width of the model. Considerations in potential flow theory indicated that a length 1.5 times the height should result in nearly horizontal streamlines at the comparable distance from the wellbore. The model performed as anticipated in this respect.

The specific gravities of the oil and of the water used in the model were 0.826 (39.8° API) and 1.0078, respectively, with corresponding viscosities of 2.18 and 0.905 cp. The calculated value of ν_{wm}/ν_{om} was 0.34. This is a typically average value to be found in the prototype. Similarly, the value of $\left[\frac{\rho_o - \rho_w}{\rho_o}\right]_m$ is -0.143, an average value to be found in oil reservoirs with a water-bearing section.

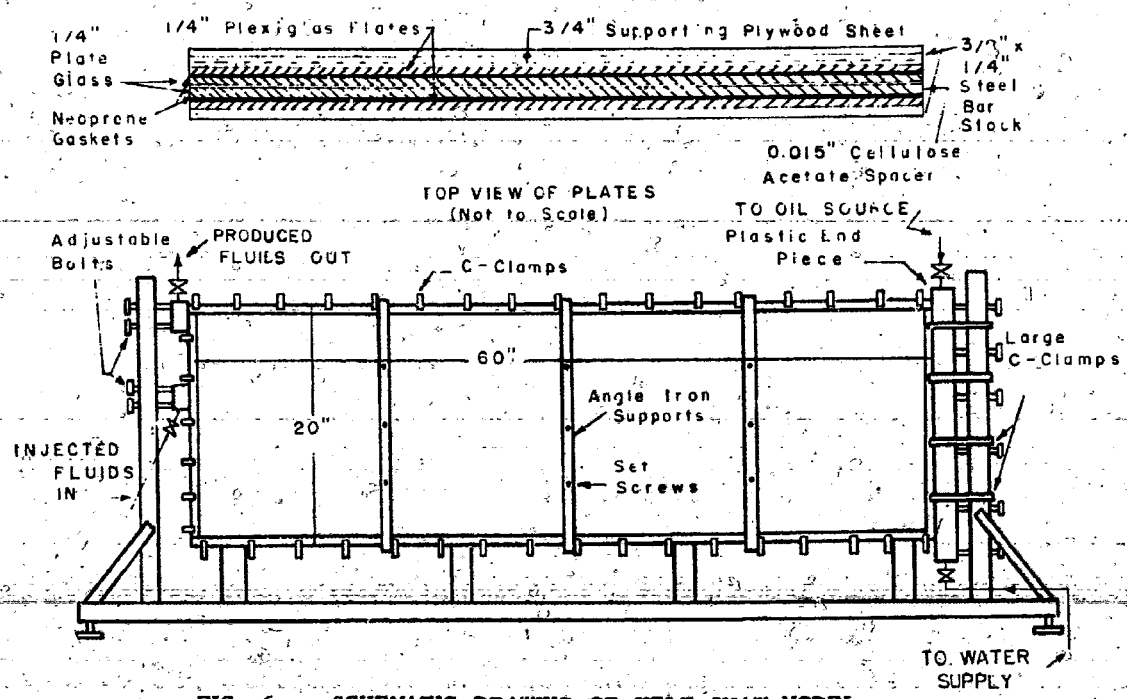

FIG. 6 — SCHEMATIC DRAWING OF HELE-SHAW MODEL.

DESIGN OF THE MODEL

Fig. 6 is a schematic drawing of the Hele-Shaw model constructed. Two pieces of ¼ in. thick plate glass, 60 in. long by 20 in. high, were used. Close spacing was accomplished along the top and bottom edges with a cellulose acetate strip 3/8 in. wide and 0.015 in. thick. In addition, ¼ in. thick plexiglas plates with appropriate gaskets were placed on both sides of the glass plates. The purpose of these plates was to provide a plexiglas-glass annular space to contain fluid subjected to approximately the same head as the fluids flowing within the glass plates. This procedure was found to be necessary to accurately control the spacing between the glass plates and to avoid breakage.

Oil and water entered the right-hand side of the model through a plastic end piece. Two smaller end pieces comprised the point of injection and the producing interval on the left side of the model. The model then represents the right side of a two-dimensional system.

Tap water and No. 2 fuel oil were used in the flow tests. To minimize capillary effects due to interfacial tension, 0.01 per cent by weight sodium hexametaphosphate was added. A dark blue oil-soluble dye was added to the fuel oil. Viscous mineral oil was used to increase the viscosity of the fuel oil for injection purposes.

EXPERIMENTAL PROCEDURE

A cone shape was established for a particular inlet-cone height by adjusting the incoming oil and water rates. This established a particular water-oil ratio. After the cone shape and stand-pipe pressures had stabilized, which required from 30 minutes to 2 hours, the flow pattern in the model was photographed. The tests normally involved injection of fluid at a point below the producing interval. To maintain the inlet-cone height constant, a specific injection rate was matched by a corresponding increase in the total fluid producing rate. The total fluid produced then consisted of the reservoir oil producing rate (always held constant throughout a test series), the injected oil and the resulting water. The resulting net water-oil ratio was calculated from the water producing rate and the reservoir oil producing rate (note that the injected oil is not included). The cone shapes were photographed.

PRESENTATION OF DATA AND RESULTS

A total of 18 different test series[5] were made with the Hele-Shaw model. Details on each of these are available as noted in the bibliography. Some of the tests will be discussed in abbreviated form.

One of the factors investigated was the influence of the viscosity of the injected oil. Fig. 7 illustrates the water cone shapes at a constant net oil producing rate of 0.5 cc/sec with an inlet cone height of 5 in. and a viscosity ratio of injected/reservoir oil of 4:1. Production was at a point sink at the extreme top of the producing interval. Curve A outlines the cone shape for zero oil injection and a water-oil ratio of 0.682. Curves B through E show the observed cone shapes for oil injection rates of 4.4, 9.3, 21.8 and 30.7 per cent, respectively, of the total oil producing rate. Note that Curve E depicts the cone shape with complete suppression of the water production. Fig. 8 summarizes the data showing the influence of the injection oil viscosity for viscosity ratios of 1, 4 and 10:1. The increase in injection viscosity is equivalent to reducing the permeability by the same factor in the area through which the

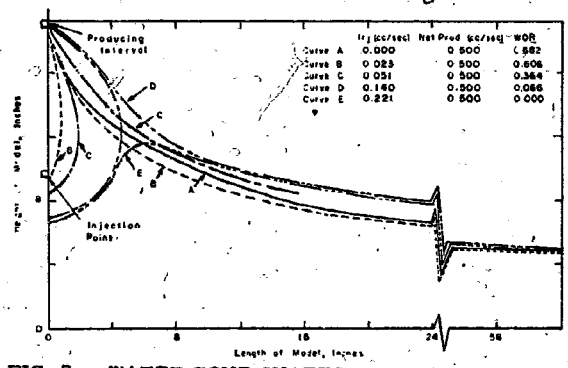

FIG. 7 — WATER CONE SHAPES — TWO-DIMENSIONAL MODEL, 5 IN. INLET CONE HEIGHT, INJECTION AT MID POINT, VISCOSITY RATIO OF INJECTED TO RESERVOIR OIL = 4.

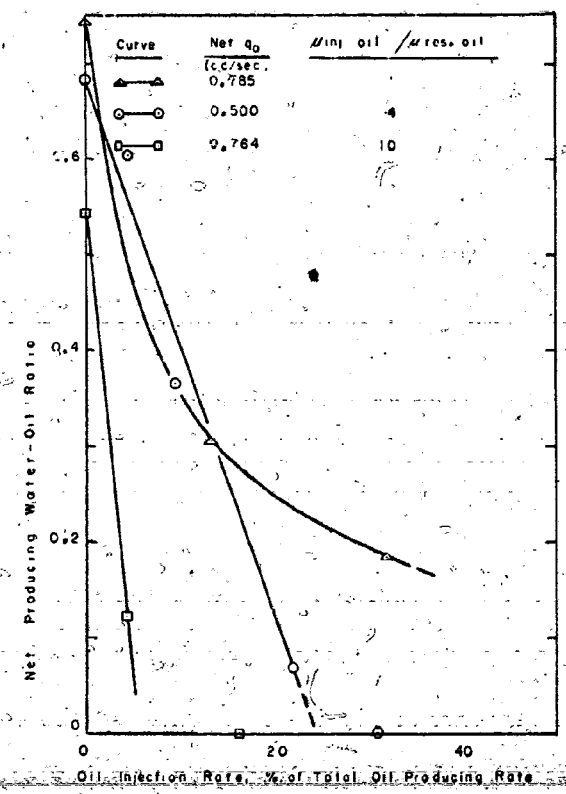

FIG. 8 — CURVES TO ILLUSTRATE THE INFLUENCE OF INJECTION OIL VISCOSITY — TWO-DIMENSIONAL MODEL, INJECTION AT MID POINT OF INTERVAL, 5 IN. INLET CONE HEIGHT.

injected fluid flows. As might be expected, smaller volumes of oil are required to reduce the net water-oil ratio as the ratio of the viscosity of the injected oil to reservoir oil is increased. The plotted points of Fig. 8 do not follow a smooth curve. This is probably because of the sensitivity of the model to small pressure changes.

A second factor of importance in the injection of fluid to control water coning is the position of the point of fluid injection. Fig. 9 shows the net producing water-oil ratio for various oil injection rates with the position of the point of injection as a parameter. Curves A and C illustrate the relative effects of oil injection rate on the net producing water-oil ratio where the net oil producing rate was held constant at 0.63 cc/sec. It was found that complete suppression of water coning was not possible at the net producing rate of 0.63 cc/sec with injection at the 7/8th point (Curve C). Further increase in injection rate would have interfered with the producing rate. Curve B corresponds to the lower net oil producing rate of 0.398 cc/sec with injection of oil at the 3/4th point of the formation.

Fig. 10 depicts the effect of the inlet cone height where the oil injection was at the 3/4 point of the reservoir. Due to model limitations, it was necessary to change the net oil producing rate with each change in the inlet cone height. From the test series[5] it can be stated that as the oil leg thickness became smaller, increasing amounts of injection oil were required for the same reduction in the net producing water-oil ratio (for the same position of the injection point).

Fig. 11 sets out the cone shapes observed when production was through a "finite" interval above a simulated cement pancake. The purpose of this test series was to determine the effect of increasing the size of the producing interval. Curve A represents the cone shape obtained for a net oil producing rate of 0.63 cc/sec. This producing rate was held constant throughout the test series. Curve B shows the cone shape obtained for an injection of 51.2 per cent of the total oil produced. The viscosity ratio was 1:1. The net producing water-oil ratio was reduced from 0.498 for zero injection to 0.37. Comparison of the results to

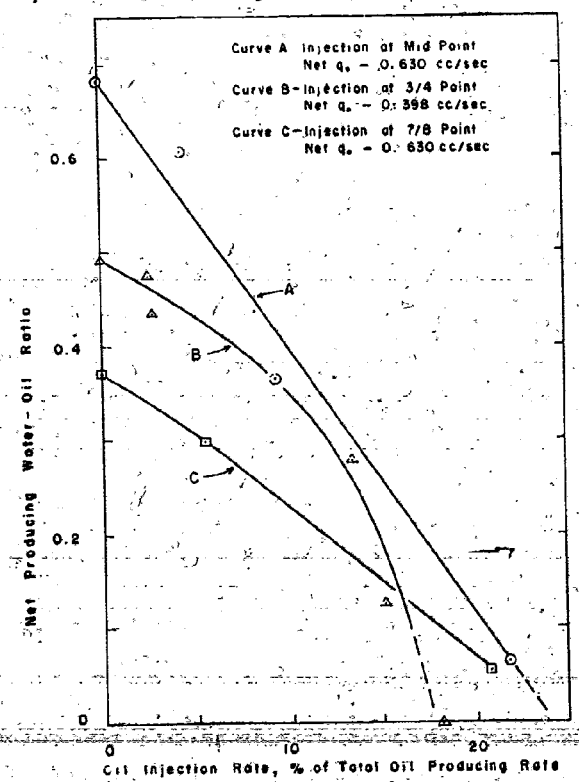

FIG. 9 — CURVES TO ILLUSTRATE THE INFLUENCE OF THE POSITION OF THE POINT OF INJECTION — TWO-DIMENSIONAL MODEL.

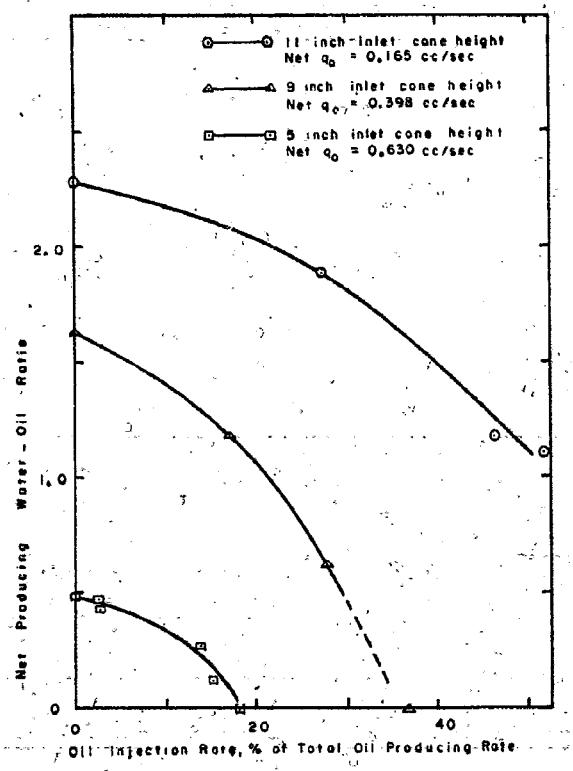

FIG. 10—CURVES TO ILLUSTRATE THE INFLUENCE OF INLET CONE HEIGHT — TWO-DIMENSIONAL MODEL, INJECTION AT 3/4 POINT OF INTERVAL, RATIO OF INJECTED TO RESERVOIR OIL VISCOSITY = 4.

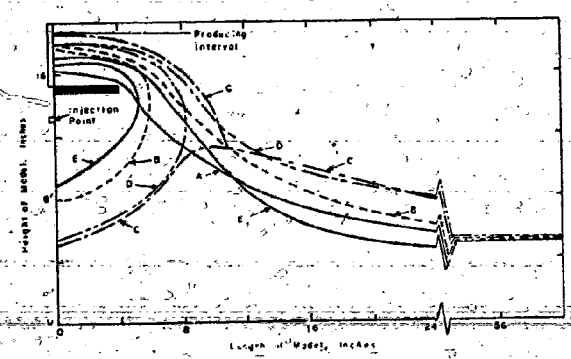

FIG. 11 — WATER CONE SHAPES — SIMULATED PANCAKE AT BOTTOM OF FINITE PRODUCING INTERVAL, OIL INJECTION.

those where no pancake was present[5] shows that for the conditions of the experiment, 0.63 cc/sec net oil producing rate and 0.597 net producing water-oil ratio, an injection rate of 51.2 per cent resulted in a net water-oil ratio of 0.37. These data indicate that little benefit from the presence of the pancake was observed for comparable injection rates.

Curves E, D, and C of Fig. 11 present the cone shapes observed for injection rates of 13.9, 30.9, and 35.8 of the 4:1 viscosity ratio oil as a per cent of the total oil producing rate. The injection rate of 35.8 per cent was sufficient to completely suppress the water production. For the case where no pancake was used, an injection rate of 47.9 per cent was successful in reducing the net producing water-oil ratio from 0.597 to 0.111. A slight advantage over the case without the pancake is observed where the pancake configuration is used. It can be observed from Fig. 11 that as the injection rate was increased, the water cusp tended to move upward on the producing interval thus making it difficult to suppress the water cone.

WATER CONING STUDY WITH THE RADIAL MODEL

THEORETICAL BASIS AND SCALING FACTORS

Radial flow in oil reservoirs can be represented in laboratory models if proper scaling procedures are followed. The physical and dynamic dimensionless groups necessary to effect such a scaling of a laboratory model to a field prototype have been adequately reported in the literature[12,13] and will not be developed here. If the values of the pertinent dimensionless groups formed from the variables of the system are the same for a model and for a prototype, then the model is properly scaled. It follows that the results of experiments made with a properly scaled model in the laboratory can be interpreted as a measure of field performance.

Since the plan was to study the effect of injection on cone shape and the resulting net producing water-oil ratio in a radial model containing unconsolidated sand, the complications of relative permeability and capillary effects were avoided by the use of miscible fluids. These fluids will be discussed in a following section. It is then evident that the only dynamic parameter necessary to characterize the system would be a ratio of the gravity and viscous forces. Henley, *et al*,[14] suggest that such a ratio would have a dimensionless value ranging from 0 to 1,000 in the field. Values of 2.9 to 3.9 of this parameter were studied in the present radial model.

Because the fluids used in the model were miscible, the mobility ratio was directly proportional to the viscosity of the water divided by the viscosity of the oil. In the field, a range of values of this parameter from 0.1 to 10 could be encountered. The fluid system used in the model had a mobility ratio of 1.21.

Four geometric parameters are of interest in this study. The first of these is the dimensionless well spacing. The equation is given in Table 1. Since a homogeneous sand pack was used, the horizontal and vertical values of the permeability are equal. For a model well-to-well spacing of 36 in., and an oil pay thickness of 8 in., the resulting value of the dimensional well spacing is 4.5.

The second geometric parameter considered is the dimensionless well radius. In the model, the screened opening to the wellbore of 0.04 in. for the 45° pie-shaped radial section, results in a wellbore radius of 0.048 in. The dimensionless expression is recorded in Table 1. Since the value of h is 8 in., the dimensionless well radius is calculated to be 6.0×10^{-3}.

Dimensionless well penetration, the third geometric parameter, is 0.0625 for the ½ in. producing interval of the model.

The fourth parameter used to describe the geometry of the system indicated the position of the point of fluid injection as a fraction of the thickness of the oil producing interval. This has been called l_D and is a ratio of c to h where c is the distance from the top of the oil producing section to the centerline of the injection interval. In the radial model, three experimental values of l_D were used, 0.156, 0.281 and 0.469. For completeness, an auxiliary value of the dimensionless depth l_D could be used. This would be a dimensionless measure of the distance from the bottom of the producing interval to the centerline of the point of injection $(c-d)$. For the three injection intervals used, the values of l'_D are 0.094, 0.219 and 0.406.

Table 1 summarizes values of the scaling parameters calculated for the radial model. It indicates the possible prototype values of the dimensionless groups and presents the equations of the parameters.

THE RADIAL MODEL

Fig. 12 is a sketch of the radial model. The geometry of the wellbore was accurately fixed by using two 1 × 2 × 12 in. plexiglas pieces. A taper of 22.5° was milled into both pieces, then producing and injecting intervals were prepared so that an opening of 0.04 in. into the model resulted. The two pieces are held together and fastened to the sides of the model with machine screws. A neoprene gasket, cut to fit the top, completed the model.

It should be noted that the model is inverted from the system found in the field. This experimental procedure was necessary to insure that the sand pack in the vicinity of the producing and injecting points be tight and uniform. Pressure applied to the top of the model above the neoprene diaphragm made certain that the pack remained tight, and that no channeling fluids across the top occurred during the test.

The sand used in the model varied in size from 60 to 200 mesh with an average mesh size of 110. The specific surface calculated on a unit pore-volume basis of the sand was 942 sq cm/cu cm.

Using a porosity of 30 per cent, the value of specific surface and Kozeny's equation for a well-rounded unconsolidated sand, a permeability of 10.6 darcies resulted.

The sand was packed wet using a vibrator and a small tamping rod. Uniformity of the sand pack was evident from the even advance of a colored fluid front through the model with continued injection.

During the tests, two positive displacement pumps were used to pump the fluids corresponding to the reservoir oil and the injection fluid. Since the model was inverted as compared to the prototype, the "reservoir oil" was admitted at the bottom of the back of the model. Because the producing interval was not at the bottom of the model on the left-hand side, the injected fluid was introduced at a higher point.

In order to avoid the complications of relative permeability and capillary pressure phenomena, miscible fluids were used. These fluids were tap water and salt water. The tap water had a specific gravity of 0.998 and a viscosity of 0.894 cp while the salt water had a specific gravity of 1.095 with a viscosity of 1.082 cp. All measurements were taken at a constant laboratory temperature of 76F.

To facilitate observation and photography of the resulting cone shapes during the tests, the salt water, which corresponds to the reservoir oil in this inverted system, was colored with brilliant blue food coloring. A small amount of mercuric chloride was added to control any possible growth of algae.

EXPERIMENTAL PROCEDURE

To avoid confusing the reader, the procedure will be outlined as if the system were not inverted and as if the salt water used were really reservoir oil.

Since the sand in the model was packed wet, the system was initially full of tap water and completely free of any residual air saturation. Reservoir oil was then admitted to the model until the tap water had been displaced to the desired inlet cone height. Throughout the tests, the inlet cone height was 4 in. To maintain this cone height with a producing water-oil ratio from the producing interval, water was introduced through an adjustable needle valve. A stable cone height would then be established under dynamic fluid flow conditions.

When the pressures and the cone shape in the system had stabilized, an 8 to 20 hour phase of each test series, the flow pattern was photographed and the flow rates recorded.

After establishing the stable cone, the tests conducted involved the injection of reservoir oil at a point below the producing interval. The total fluid produced consisted of the reservoir oil, the injected oil and the resulting produced water. Since all fluids were miscible, it was necessary to determine the per cent of salt water (the reservoir oil) by means of density difference. As all the fluid rates were then known, the net producing water-oil ratio could be calculated from the water producing rate and the reservoir oil producing rate (note that the injected oil is not included). A suitable basis then existed for comparison to the water-oil ratio obtained without injection.

TABLE 1 — SCALING PARAMETERS FOR THE RADIAL MODEL AND THE PROTOTYPE

Dynamic Parameters	Radial Model	Possible Prototype**
(i) Gravity to Viscous Force Ratio $R_3 = \frac{q(\rho_w - \rho_o)^*}{q\mu_o/k_v A}$	4.5	0 to 1,000
Rock & Fluid Property Parameter		
(i) Mobility Ratio, $M = \frac{k_o \mu_w}{k_w \mu_o}$	1.21	0.1 to 10
Geometric Parameters		
(i) Dimensionless Well Spacing, $a_D = \frac{a}{h}\sqrt{\frac{k_v}{k_h}}$	4.5	2 to 20
(ii) Dimensionless Well Radius, $r_{wD} = \frac{r_w}{h}\sqrt{\frac{k_v}{k_h}}$	6×10^{-3}	8×10^{-5} to 2×10^{-1}
(iii) Dimensionless Well Penetration, $b_D = \frac{b}{h}$	0.0625	0 to 1
(iv) Dimensionless Injection, $l_D = \frac{c}{h}$	0.156 to 0.469	0 to 1
or, $l_D = \frac{c-d}{h}$	0.094 to 0.406	0 to 1

*q as used refers to flow rate of fluids exclusive of injected fluids
** as suggested by Henley, et al[14]

EXPERIMENTS CONDUCTED AND ANALYSIS OF RESULTS

The purpose of this test series was to determine the shape of the stable water cone for the model, to determine the change in cone shape with fluid injection, and to ascertain the resulting net water-oil ratios for various oil injection rates. Fig. 13 shows the resulting cone shapes. Curve A represents the interface between the oil and water for stable flow conditions with zero oil injection and a net oil producing rate of 0.13 cc/sec. Curves B, C and D show the resulting cone shapes for injection rates of 11.4, 34.4 and 50.7 per cent, respectively, of the total oil producing rate.

The upper curve of Fig. 14 is a plot of the net producing water-oil ratio vs the oil injection rate as a per cent of the total oil producing rate corresponding to the model configuration of Fig. 12. It can be observed that while a significant reduction in the producing water-oil ratio was effected by the injection of a 1:1 viscosity ratio of injected and reservoir oils, the point of oil injection was too low.

The middle and lower curves of Fig. 14 correspond to model configurations where the point of oil injection has been moved closer to the producing interval. It can be observed that injection at the higher points has been more effective in reducing the water-oil ratio for a given rate of oil injection. In addition, the cross-sectional area through which the water must move has been reduced with increased oil injection rates.

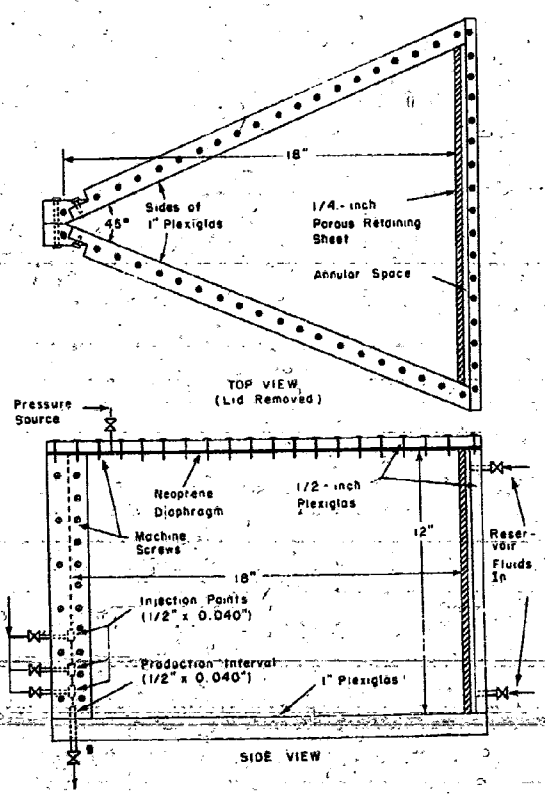

FIG. 12 — SKETCH OF RADIAL MODEL.

GENERAL DISCUSSION

A striking and very important fluid flow feature can be observed by comparing the cone shapes of Figs. 5 and 13. A marked similarity is evident in cone shapes and injection profiles in the analytically derived and experimentally determined flow systems. It might have been expected that the cone in the radial system would have been very steep in slope near the producing interval. This was not observed. The above observation indicates that the results of analytical treatments of the water coning problem in two-dimensions have qualitative application to the radial system most often encountered in the field prototype.

The situation is a fortuitous one since a radial system is most difficult to treat either in the laboratory or by analytical means. The positioning of impermeable barriers or pancakes is very difficult in a radial system. The system must be unpacked, then repacked. Invariably, the system would be substantially altered and correlation of the test

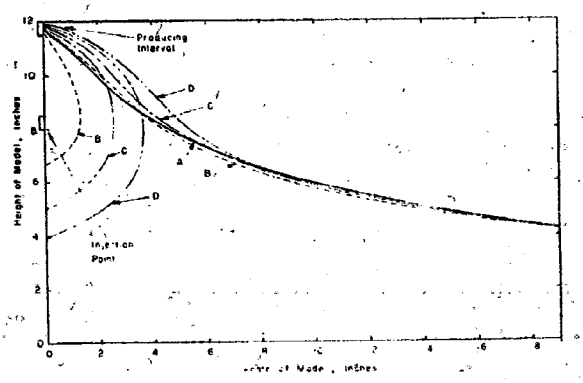

FIG. 13 — WATER CONE SHAPES — RADIAL FLOW MODEL, I_D = 0.469, NET OIL PRODUCING RATE 0.13 CC/SEC, VISCOSITY RATIO OF INJECTED TO RESERVOIR OIL = 1.

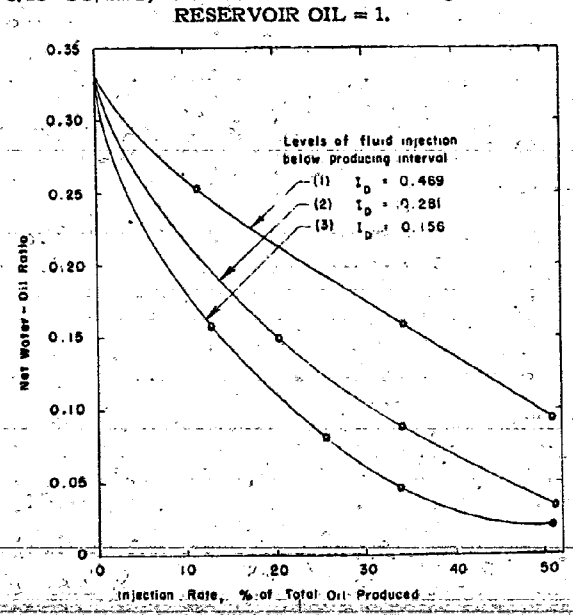

FIG. 14 — NET WOR VS FLUID INJECTION RATE — RADIAL FLOW MODEL, NET OIL PRODUCING RATE 0.13 CC/SEC, VISCOSITY RATIO OF INJECTED TO RESERVOIR OIL = 1.

results to previous tests could not be made. Studies conducted using the Hele-Shaw model do not have this disadvantage.

The concept of fluid injection to suppress or partially suppress water coning should be directly applicable to field operations. The formation type, the condition of the wellbore, and the formation fluid characteristics will have an all important bearing as to whether such a project would be workable on an individual application basis. It may be readily observed that the fluid used for injection need not be reservoir oil. The fluid could be reservoir oil treated with a compound to increase viscosity. Smaller volumes of oil would then be required to reduce the net water-oil ratio. The increase in injection fluid viscosity is equivalent to reducing the permeability by the same factor in the area through which the injected fluid flows.

Reinjecting produced salt water to effect cone suppression should be both feasible and advisable in some formations. Where a salt water disposal well is required, this approach to water disposal and suppression of water coning might be attractive economically. The viscosity of the salt water could be increased by chemical means when necessary.

CONCLUSIONS

From the analytical development and experimental work of this study,[5] the following conclusions may be drawn in regard to fluid injection as a means of preventing or partially preventing water coning in oil wells.

1. The use of two-dimensional model techniques permits qualitative conclusions regarding water coning behavior in a radial system.
2. The smallest water-oil ratio will result when the smallest possible producing interval, consistent with the required fluid producing capability, is placed at the top of the oil zone.
3. The net producing water-oil ratio for a given oil producing rate can be reduced by the injection of fluid. More benefit is derived if the injection fluid is more viscous than the reservoir oil, or if a zone of reduced permeability exists in the vicinity of the point of fluid injection.
4. For a given net oil producing rate, the optimum point of fluid injection will be the point closest to the bottom of the producing interval that does not interfere with the desired oil producing rate. This means that for higher net oil producing rates, the point of injection should be moved downward for maximum efficiency in water cone suppression.
5. The same cone shapes and net producing water-oil ratios will result regardless of the sequence of operations followed, as long as sufficient time has elapsed for steady-state conditions to be reached. This means that no advantage resulted from initiating fluid injection before the water cone was developed or vice versa (see Ref. 5).
6. When no fluid is injected, the water cone shape is virtually independent of the oil producing rate (see Ref. 5).

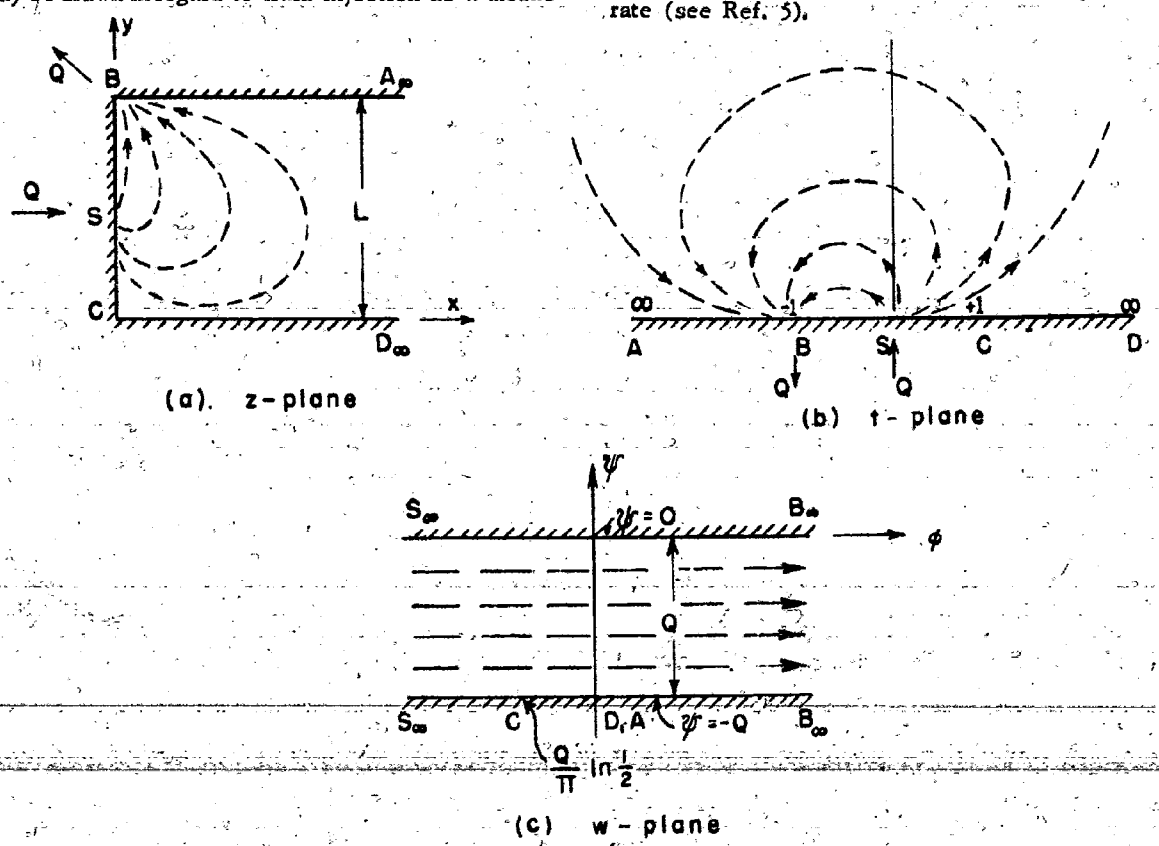

FIG. 15 — DIAGRAMS FOR CONFORMAL TRANSFORMATIONS.

7. The reduction in the net producing water-oil ratio, attributable to the use of simulated pancakes, was minor in the model studies conducted.

8. The injected fluid will not be lost if the fluid is less dense than the connate water of the reservoir.

9. The conformal mapping technique used for the analytical treatment of the zero fluid density difference case with fluid injection, should permit qualitative determination of the fluid injection behavior and the accruing benefits to be realized in a radial system.

NOMENCLATURE

a = Well-to-well distance, in. or ft,

c = Distance from top of oil pay to centerline of injection, point, in. or ft,

D = Production interval, in. or ft,

I_D = Dimensionless injection depth,

u, v, w = Velocity components in the x, y, z directions, respectively,

ν = Fluid specific gravity,

Q = Dimensionless flow rate,

L = Height of the system.

REFERENCES

1. Muskat, M. and Wyckoff, R. D.: "An Approximate Theory of Water-Coning in Oil Production", *Trans.*, AIME (1935) Vol. 114, 144.
2. Meyer, H. I. and Garder, A. O.: "Mechanics of Two Immiscible Fluids in Porous Media", *Jour. of Appl. Phys.* (Nov., 1954) 1400.
3. Pirson, S. J.: *Oil Reservoir Engineering*, McGraw-Hill Book Co., N. Y. (1958) 432.
4. Shul'ga, P. M.: "Approximate Formula for the Maximum Production Rate of Water-Free and Gas-Free Oil from a Formation Carrying Bottom Water and a Gas Cap", *Izvest. Vysshikh Uchzb. Zaved.*, Neft i Gaz (1959) Vol. 2, No. 7, 33.
5. Smith, C. R.: *Water Coning Control in Oil Wells by Fluid Injection*, Ph.D. Thesis, U. of Texas (Aug., 1962).
6. West, T. S.: "A Gravel Pack Completion for Exclusion of Gas and Water", *Trans.*, AIME (1951) Vol. 192, 183.
7. Vallentine, H. R.: *Applied Hydrodynamics*, Butterworth and Co., Ltd., London (1959).
8. Karp, J. C., Lowe, D. K. and Marusov, N.: "Horizontal Barriers for Controlling Water Coning", *Jour. Pet. Tech.* (July, 1962) XIV, 783.
9. Hele-Shaw, H. S. and Hay, A.: "Streamline Motion of a Viscous Film", British Assoc. Report – Bristol Meeting (1898) Sec. A.
10. Hele-Shaw, H. S. and Hay, A.: "Lines of Induction in a Magnetic Field", *Phil. Trans.* Series A) 195, 303.
11. Bear, J.: "Scales of Viscous Analogy Models for Ground Water Studies", *Jour. Hyd. Div. ASCE* (Feb., 1960) 11.
12. Geertsma, J., Croes, A. and Schwarz, N.: "Theory of Dimensionally Scaled Models of Petroleum Reservoirs", *Trans.*, AIME (1956) Vol. 207, 118.
13. Rapoport, L. A.: "Scaling Laws for Use in Design and Operation of Water-Oil Flow Models", *Trans.*, AIME (1955) Vol. 204, 143.
14. Henley, D. H., Owens, W. W. and Craig, F. R.: "A Scale Model Study of Bottom-Water Drives", *Jour. of Pet. Tech.* (Jan., 1961) XIII, 90.
15. Rouse, H.: *Advanced Mechanics of Fluids*, John Wiley & Sons Inc., N. Y. (1959) 189.

APPENDIX

DERIVATION: FLOW FROM MID-POINT TO ADJACENT CORNER IN A CHANNEL

For determination of the complex potential, the configuration pattern in the z-plane is transformed to the upper half of the t-plane. The t-plane flow is that of flow away from a half-source at the origin to a half-sink at $t = -1$. Further transformations yield parallel flow in an infinite strip on the w-plane.

z-plane to t-plane:

Using the Schwarz-Christoffel theorem,[15] the polygon of the z-plane is transformed into the real axis of the t-plane. The transformation in integral form is:

$$a = E\int \frac{dt}{(a-t)^{\alpha/\pi}\,(b-t)^{\beta/\pi}\,(c-t)^{\gamma/\pi}\,(d-t)^{\delta/\pi}} + F \quad \ldots\ldots\ldots\ldots \quad (11)$$

where: $E = R_e^{i\theta}$, a complex constant

a, b, c, d are real constants in increasing order of size

$\alpha, \beta, \gamma, \delta$ are external angles of the polygon

F = complex constant of integration fixing the position of the origin.

Applying Eq. 11 to the semi-infinite strip of the z-plane, A is placed at $-a$ in the t-plane, the points B and C at $t = -1$ and $t = 1$, respectively, and D remains at $t = a$. Eq. 9 becomes:

$$z = E\int \frac{dt}{\sqrt{(-1-t)\,(1-t)}} + F \quad \ldots\ldots \quad (12)$$

Integrating Eq. 12 and evaluating E and F to have values of L/π and zero, respectively, results in the transformation equation:

$$t = \cosh\frac{\pi z}{L} \quad \ldots\ldots\ldots\ldots \quad (13)$$

t-plane to w-plane:

The point $t = 0$ is regarded as a source with a total flow of $2Q$ of which half goes to the upper half of the t-plane. Similarly, $t = -1$ a sink of the total flow $2Q$. For this source-sink combination:

$$W = \frac{2Q}{2\pi}\ln t - \frac{2Q}{2\pi}\ln(t+1) = \frac{Q}{\pi}\ln\frac{t}{t+1} \quad . \quad (14)$$

This equation represents parallel flow in an infinite strip in the w-plane as shown in Fig. 15. Combining Eqs. 13 and 14 results in the complex potential equation for flow in the z-plane:

$$W = \frac{Q}{\pi} \ln \frac{\cosh \frac{\pi z}{L}}{\cosh \frac{\pi z}{L} + 1} \quad \ldots\ldots\ldots \quad (15)$$

Taking the real and imaginary parts of Eq. 15 and equating them to ϕ and ψ, respectively, results in analytic expressions for the potential and stream functions:

$$W = \phi + i\psi = \frac{Q}{\pi} \ln \frac{\cosh\left[\frac{\pi x}{L} + \frac{i\pi y}{L}\right]}{\cosh\left[\frac{\pi x}{L} + \frac{i\pi y}{L}\right] + 1} \quad \ldots \quad (16)$$

Equating of the real and imaginary parts of the above equation after some algebraic manipulation results in the following expressions:

$$\phi = \frac{Q}{2\pi} \ln \left[\cos^2 \frac{\pi y}{L} + \sinh^2 \frac{\pi x}{L}\right]$$

$$\frac{-Q}{2\pi} \ln \left[\left\{\cosh \frac{\pi x}{L} \cos \frac{\pi y}{L} + 1\right\}^2 + \sinh^2 \frac{\pi x}{L} \sin^2 \frac{\pi y}{L}\right] \quad \ldots\ldots\ldots \quad (17)$$

$$\psi = \frac{Q}{\pi} \arctan \left[\tanh \frac{\pi x}{L} \tan \frac{\pi y}{L}\right]$$

$$\frac{-Q}{\pi} \arctan \left[\frac{\sinh \frac{\pi x}{L} \sin \frac{\pi y}{L}}{\cosh \frac{\pi x}{L} \cos \frac{\pi y}{L} + 1}\right] \quad \ldots \quad (18)$$

***